Int. J. Electrochem. Sci., 10 **(2015)** 1595 - 1615

International Journal of
ELECTROCHEMICAL
SCIENCE
www.electrochemsci.org

Environmentally Safe Protection of Carbon Steel Corrosion in Sulfuric Acid by Thiouracil Compounds

F. El-Taib Heakal[1,*], *A.S. Fouda*[2], *S.S. Zahran*[3]

[1] Department of Chemistry, Faculty of Science, Cairo University, Giza,12613, Egypt
[2] Department of Chemistry, Faculty of Science, El-Mansoura University, El-Mansoura, 35516, Egypt
[3] Petrogulf Misr Company, Maadi, Cairo, Egypt
[*]E-mail: feltaibheakal@gmail.com; fakihaheakal@yahoo.com

Received: 4 November 2014 / *Accepted:* 15 December 2014 / *Published:* 30 December 2014

The inhibitive effect of three thiouracil (TU) compounds on protecting carbon steel corrosion in sulfuric acid was investigated. Experimental results showed that inhibition efficiency of 6-methyl-2-thiouracil (TU-I) is higher than that for 2-thiouracil (TU-II) or 6-phenyl-2-thiouracil (TU-III), i.e. TU-I > TU-II > TU-III. The inhibition efficiency increases with concentration and decreases with temperature. Potentiodynamic curves showed that tested thiouracils are of mixed type inhibitors. Values of charge transfer resistance (R_{ct}) and double layer capacitance (C_{dl}) were estimated from impedance data. Thermodynamic functions for the corrosion process were obtained to glean the inhibition mechanism. The adsorption of inhibitors obeys Temkin isotherm. Synergistic effect brought about by the combination of each inhibitor and KI, KBr or KCl was also investigated. The corrosion inhibition process was discussed from the perspective of theoretical properties of the compounds: E_{HOMO}, E_{LUMO}, $\Delta = E_{HOMO} - E_{LUMO}$ and dipole moment (μ), their values confirm the inhibition data.

Keywords: Carbon steel; Corrosion inhibitors; Thiouracils; Weight loss; Polarization; EIS

1. INTRODUCTION

The corrosion of iron and steels is a fundamental academic and industrial concern that has received a considerable amount of attention. In particular, carbon steel is a common constructional material for many industrial units because of its cost and excellent mechanical properties [1]. However, it suffers sever attack, especially in oil and gas production systems, as well as in acid environments [2]. Mineral acid solutions are widely used in many industrial processes due to their special chemical properties. The most important fields of application being acid pickling, industrial acid cleaning, acid descaling and oil-well acidizing [3,4]. Because of the general aggressiveness of

acid environments, the strategy is to isolate the metal from the corrosive agents [4]. The use of inhibitors is one of the most practical methods adopted for protecting metallic constructions against corrosion, especially in acid media [5]. Numerous studies on corrosion inhibition using heterocyclic organic compounds have been reported [6-16]. It has been accepted that most organic inhibitors adsorb on the metal surface by displacing water molecules over there and forming a compact barrier film. The inhibitor adsorption mode was strictly dependent on the electronic structure of the molecules due to the presence of appropriate functional groups, aromacity, electron density at the donor atoms and π orbital character of donating electrons [9,17] . The inhibitor films can be classified as (i) a chemisorbed film donating a lone pair of electrons attached to a central adsorption atom in a functional group, (ii) an electrostatic adsorption film or as (iii) a precipitation and/or a complex film resulting from the reaction of dissolved metal ion and organic inhibitor molecule [17]. Ajmal et al. [18] reviewed the use of heterocyclic compounds as corrosion inhibitors for acid media. It was suggested that sulfur-containing compounds and nitrogen-containing compounds are effective inhibitors for sulfuric acid corrosion. Compounds containing both S, N were found to be better inhibitors than those containing either atom alone [19].

Our earlier study using uracil and adenine as natural green inhibitors for the corrosion of Sn-Ag binary alloy in acidic media has demonstrated that there is a correlation existing between the inhibition efficiency and molecular structure [20]. It was found that these two environmentally safe compounds experience good inhibitive efficacy in nitric acid corrosive media and the inhibition efficiency may be explained in terms of their electronic properties. The aim of the present work is devoted to investigate the inhibitive performance of three thiouracils, namely, 6-methyl-2-thiouracil (TU-I), 2-thiouracil (TU-II) and 6-phenyl-2-thiouracil (TU-III) for carbon steel corrosion in the aggressive sulfuric acid medium. The choice of these inhibitors was based on the fact that they contain lone pairs of electrons and hetero atoms such as N, O, and S, which invoke greater adsorption of inhibitor molecules on the steel surface. Also, the synergistic action of halides on the corrosion process behavior is investigated. The study is complemented with theoretical quantum chemical calculations in order to provide an explanation for the differences between the probed and the impact of their molecular structures.

2. EXPERIMENTAL

2.1. Materials

Carbon steel sheets with chemical composition in mass fraction (%) : 0.200 C, 0.350 Mn, 0.024 P, 0.003 Si and the remainder Fe, were obtained from petroleum pipe line, Petrogulf Misr, Egypt. Before each experiment, sample surface was mechanically abraded by different grade of emery paper beginning from 400 until 1200 grit, ultrasonically degreased with acetone, rinsed with double distilled water and finally dried between two filter papers at room temperature. An aggressive acid solution was prepared by dilution of an analytical grade reagent concentrated H_2SO_4 with double distilled water. Thiouracil compounds studied in the present work are all of analytical grade reagent (Merk and

or/BDH) and used without any further purification. The structures of the tested compounds are as given in the following scheme.

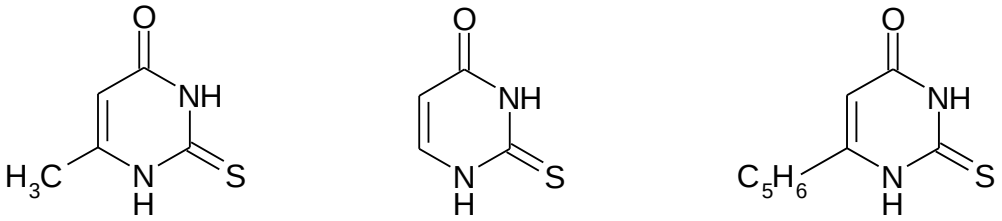

6-CH_3-2-thiouracil (I) **2-thiouracil (II)** **6-ph-2-thiouracil (III)**

Scheme 1. Structure of the tested compounds.

2.2. Chemical method

The reaction basin used in each weight loss experiment was a graduated glass vessel with 6 cm inner diameter and containing a total volume of 250 ml stagnant aerated solution under investigation . Test coupon was cut from carbon steel sheet to have nearly 2 cm × 2 cm × 0.1 cm dimensions. Prior to each experiment, the coupon was prepared as per above and then weighted using an analytical balance with precision of ± 0.1%. The test pieces were totally suspended by suitable glass hooks and rods at the edge of the basin under the surface of the test solution by about 2 cm. After specified time intervals, three test coupons were taken out of the test solution, rinsed in double distilled water, dried and weighed again and the mean value of weight loss has been reported. The standard deviation of the observed weight loss was ± 1%. The specific weight loss of the coupon before and after immersion was determined and used to calculate the corrosion inhibition efficiencies (IE_w) from the relation [21]:

$$IE_w = \frac{w - w'}{w} \times 100\,\% \qquad (1)$$

where w and w' are the weight loss (mg cm^{-2}) of carbon steel dissolution in 1.0 M H_2SO_4 without and with thiouracil additions at the desired concentrations range (1.0-13 μM) after 3 h immersion.

2.3. Electrochemical methods

A conventional three-electrode glass cell was used for all electrochemical measurements with a platinum counter electrode (CE) and a saturated calomel electrode (SCE) coupled to a fine Luggin capillary as the reference electrode, to which all potentials were referred. The working electrode (WE) was cut from carbon steel sheet under investigation and embedded in a glass tube with an epoxy resin leaving a cross sectional area of 1 cm^2 exposed to the electrolyte. The WE was left immersed in solution under open circuit condition for 30 min to attain a steady state open circuit potential (OCP) value. Both cathodic and anodic potentiodynamic polarization curves were recorded over the potential

range -900 to -300 mV vs. SCE at a scan rate of 1.0 mV s^{-1} using Weking potentiostat-galvanostat model-PGS95 and a LINSEIS model Ly 1600-IIXYt recorder. The corrosion current density (i_{corr}) was obtained by extrapolating the linear segments of cathodic and anodic log*i* vs. potential curves, from which IE was calculated using the formula [22]:

$$IE_i = \frac{i_{corr} - i'_{corr}}{i_{corr}} \times 100 \quad (2)$$

where i_{corr} and i'_{corr} are the estimated corrosion current densities in the absence and presence of inhibitor, respectively.

Linear polarization resistance (LPR) measurements were carried out from a cathodic potential of -0.025 V to an anodic potential of +0.025 V with respect to the OCP at a scan rate of 0.125 mV s^{-1} to study the effect of additives on the polarization resistance (R_p) of carbon steel in 1.0 M H_2SO_4. The R_p values were calculated from the slopes of potential vs. current linear curves in the vicinity of the free corrosion potential (E_{corr}) and IE_p was evaluated as follows [23]:

$$IE_p = \frac{R'_p - R_p}{R'_p} \times 100\% \quad (3)$$

where R_p and R'_p are the polarization resistance values in the absence and presence of inhibitor, respectively.

Electrochemical impedance spectroscopy (EIS) was performed with IM6e electrochemical workstation, Zahner elektrik, Germany, controlled by Thales software and a personal computer. EIS measurements were traced at the OCP over the frequency range 100 kHz down to 0.5 Hz by superimposing ac voltage of 10 mV amplitude peak to peak to perturb the system. Prior each experiment the WE was left immersed 30 min in the corrosive medium to reach a steady potential value. EIS data are given in the form of both Nyquist and Bode formats.

3. REULTS AND DISCUSSION

3.1. Weight-loss technique

Fig. 1 shows a typical example for the variation of weight loss of carbon steel in mg cm^{-2} at various time intervals in the absence and presence of 1.0–13 μM of 2-thiouracil (TU-II) compound. The curves obtained in the presence of different concentrations from the additive fall significantly below that of the free acid. Similar behaviors were obtained for the other two inhibitors (TU-I) and (TU-III). Values of IE_w (in %) were calculated and listed in Table 1.

Table 1. %IE of carbon steel dissolution after 30 min immersion in 1.0 M H_2SO_4 containing different concentrations from each of the three tested inhibitors at 30 ^oC.

[inhibitor] $\times 10^6$ (M)	TU-I	TU-II	TU-III
1	35	25	15
3	45	35	21
5	51	45	31
7	63	55	41
9	70	65	51
11	75	71	61
13	81	78	63

In all cases, increase in inhibitor concentration from 1.0 μM to 13 μM is accompanied by a decrease in the weight loss and an increase in IE_w.

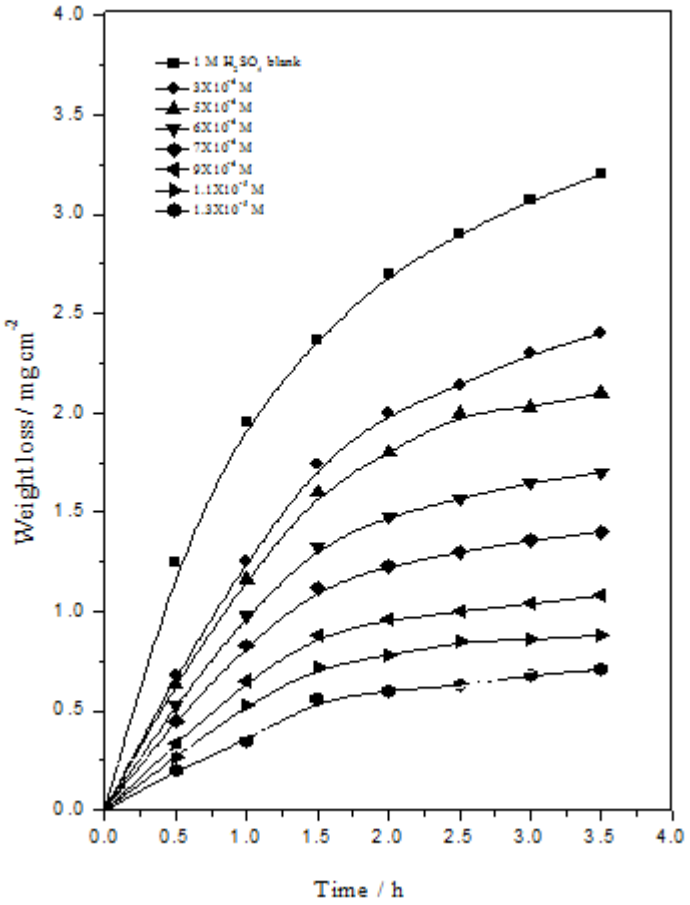

Figure 1. Weight loss-time curves carbon steel dissolution in 1.0 M H_2SO_4 solutions containing different concentrations from TU-II inhibitor at 30 ^oC.

For example, IE_w for inhibitor (I) increases from 35% at 1.0 μM to a maximum of 81% at 13 μM, and further increase in the inhibitor concentration above 13 μM was found to cause no appreciable increase in the inhibitor performance. These results lead to the conclusion that thiouracil

compounds under investigation are fairly efficient inhibitors for carbon steel dissolution in the corrosive H_2SO_4 medium and the optimum concentration is 13 μM. Careful inspection of the results shows that at any given inhibitor concentration, the ranking of the inhibitors according to their *IE* values is: TU-I > TU-II > TU-III. This indicates that 6-methyl-2-thiouracil (TU-I) exhibits the best inhibitive performance among these additives.

It is well-known that the effectiveness of an organic compound as corrosion inhibitor depends upon its molecular structure which determines its adsorption behavior on the metal surface. Inhibition of carbon steel corrosion in sulfuric acid solution by TU compounds can be explained on the basis of molecular adsorption. In fact, the adsorption of corrosion inhibitor molecules on a metal surface is the first step in the mechanism of their inhibition. Adsorption depends on both the nature and state of surface, as well as on the adsorbate properties. It is apparent from the molecular structures (cf. Scheme 1) that the tested compounds are all able to establish coordinative interactions between the free N electron pairs, eventually enforced by the π electron of the hetero ring donations and the oxidized metal surface. This restrains the corrosive attack of the aggressive medium [23]. Also, simultaneous interaction of the protonated species cannot be excluded. The existence of –SH group in the molecular structure with other substituent like the methyl group (-CH_3) as in TU-I compound can reinforce the adsorption, by increasing the effective electron density at the functional group of the additive, thereby enhances the extent of its inhibition.

3.2. Synergism

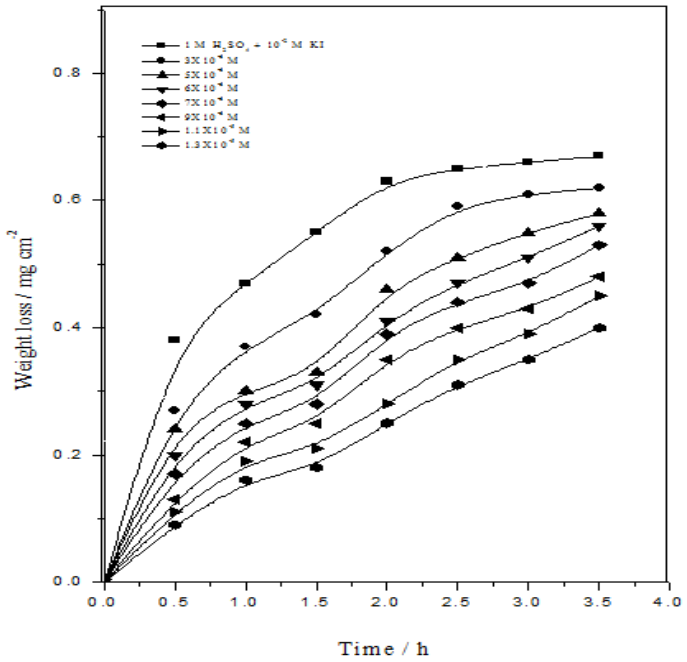

Figure 2. Weight loss-time curves carbon steel dissolution in 1.0 M H_2SO_4 + 0.01 M KI solutions containing different concentrations from TU-II inhibitor at 30 ^oC.

The corrosion behavior of carbon steel in 1.0 M H_2SO_4 solution containing lower addition (0.01 M) from KI, KBr or KCl with different concentrations from each selected inhibitor was also

examined using weight loss method. Fig. 2 is a typical example for the results obtained with various concentrations from TU-II compound + 0.01 M KI addition as a function of the exposure time. Compared with the results in absence of KI (Fig. 1 and Table 1), it is clear that combination of TU molecules and KI has better inhibition efficiency, indicating synergistic interaction between them. Addition of the other tested halides exhibits also similar behavior, where at any given inhibitor concentration the synergistic action of the halide ions decreases in the order: I^- > Br^- > Cl^-, in agreement with other findings [13,24,25]. Data of %*IE* estimated are summarized in Tables 2. It was observed from these results that halide addition decreases the corrosion rate of carbon steel sample and improves the %*IE* significantly. The interactions of these additives with the inhibitor molecules can be described by introduction of the synergistic parameter (S_θ) which is defined as [23,26,27]:

$$S_\theta = \frac{1 - \theta_{1+2}}{1 - \theta'_{1+2}} \quad (4)$$

where $\theta_{1+2} = (\theta_1 + \theta_2) - (\theta_1\ \theta_2)$, θ_1 and θ_2 are the degrees of surface coverage in presence of the halide ion (X^-) and TU molecule, respectively, and θ'_{1+2} is the measured surface coverage in presence of both species. Note that the degree of surface coverage (θ) was determined from the weight loss data (θ = %*IE*/100). S_θ approaches unity when no interaction takes place between the inhibitor molecules and the halide ion. At $S_\theta > 1$ a synergistic effect is obtained as a result of a cooperative adsorption. In case of $S_\theta < 1$, antagonistic behavior prevails due to competitive adsorption [28].

Table 2. (a) %*IE* and (b) synergism parameter (S_θ) of carbon steel after 30 min immersion in 1.0 M H_2SO_4 solution containing 0.01 M KI, KBr or KCl with different inhibitor concentrations at 30 ^oC.

Additive	[inhibitor] $\times 10^6$ (M)	TU-I		TU-II		TU-III	
		a	b	a	b	a	b
KI	1	52	1.04	36	1.04	18	1.05
	3	57	1.04	45	1.03	26	1.04
	5	65	1.00	52	1.04	34	1.15
	7	71	1.03	58	1.07	47	1.10
	9	78	1.13	69	1.09	63	1.07
	11	84	1.15	74	0.95	66	1.19
	13	89	1.18	81	1.11	68	1.12
KBr	1	48	1.05	32	1.02	19	0.90
	3	53	1.06	40	1.06	23	1.05
	5	60	1.07	48	1.05	33	1.08
	7	65	1.08	56	1.11	43	1.05
	9	72	1.07	68	1.11	60	1.09
	11	78	1.18	73	1.11	64	1.12
	13	84	1.15	80	1.17	66	1.25

	1	45	1.01	30	1.00	18	1.01
	3	50	1.04	38	0.96	23	1.00
	5	58	0.92	45	1.03	33	1.04
KCl	7	63	1.05	53	1.04	44	1.07
	9	70	1.07	66	1.06	58	1.12
	11	75	1.04	72	1.07	62	0.95
	13	80	1.17	79	1.10	65	1.10

Estimated values of S_θ given in Tables 2 are more than unity, suggesting that the phenomenon of synergism exists between the inhibitor molecules and the halide ion added. To explain the synergistic action observed between an anion and a cation Aramaki [29,30] has proposed that for competitive adsorption, the two species are adsorbed at different sites on the electrode surface. On the other hand, for cooperative adsorption, the anion is chemisorbed on the surface and the cation is adsorbed on the layer of the anions. The strong chemisorption of X^- ions (I^-, Br^- or Cl^-) on the metal surface is responsible for the synergistic effect of these ions in attraction with protonated inhibitor [31]. Surface charge is changed to negative by the specific adsorption of these ions on the metal, resulting in the joint adsorption of anions with the inhibitor cations. The inhibitors are believed to be adsorbable, not only on the cathode areas by coulombic attraction via the charge part of the protonated molecule, but also on the anode areas by a virtue of donation of the electron-pair on the nitrogen atom of the unprotonated molecule [26]. Thereby, interference adsorption can take place at the anode area.

Indeed, halide ions are good ligands because they exhibit a low electronegativity (less than 3.5) [32]. The observed trend of decrease in the synergistic action in the order $I^- > Br^- > Cl^-$, parallels the increase in their electronegativity from I^- to Cl^- (I^- = 2.5, Br^- = 2.8, Cl^- = 3.0), whilst their atomic radius decreases from I^- to Cl^- (I^- = 135 pm, Br^- = 114 pm, Cl^- = 90 pm). These facts indicate that iodide ion is more predisposed to adsorption than bromide and chloride ions, and that both the radius and electronegativity of the halide ions have a profound role on their adsorption process. Stabilization of the adsorbed halide ions by means of interaction with TU molecules leads to greater surface coverage and thereby greater protection efficacy.

3.3. Adsorption isotherms

Adsorption isotherms can provide the basic information on the interaction between the inhibitor and the steel surface. Attempts were made to fit the degree of surface coverage (θ) determined by weight loss to various isotherms including Frumkin, Langmuir, Temkin, Freundlich, Bockris-Swinkel and Flory-Huggins isotherms. The best fit for the present experimental data of TUs alone on carbon steel was attained with Temkin isotherm which is given by Eq. (7) [33,34]:

$$exp(-2a\theta) = K_{ads}\, C_{inh} \qquad (5)$$

where θ is the degree of surface coverage, C_{inh} is the inhibitor concentration, a is the lateral interaction

parameter between the adsorbed molecules and K_{ads} is the equilibrium constant for the adsorption-desorption process.

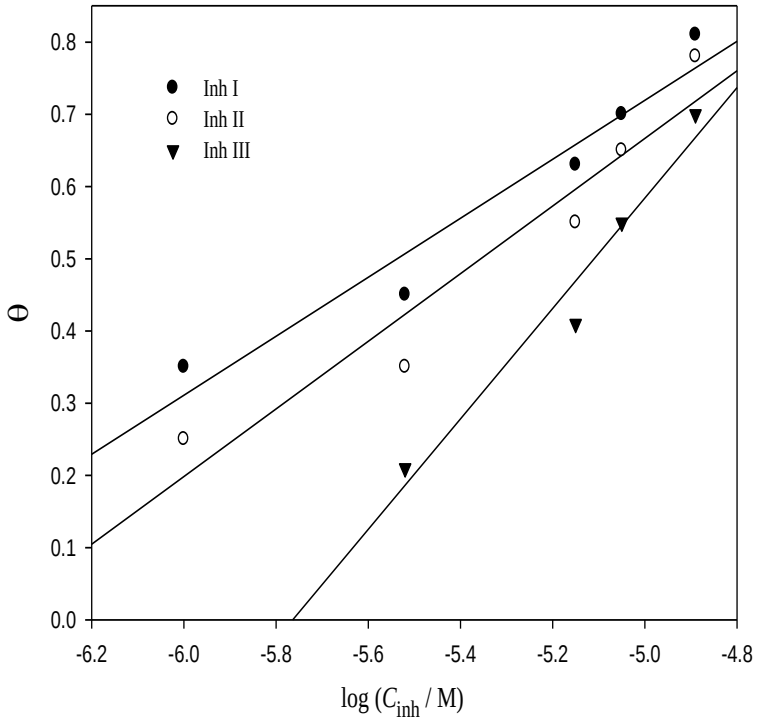

Figure 3. Temkin adsorption isotherm for carbon steel in 1.0 M H_2SO_4 solutions containing different concentrations from the three inhibitors at 30 ^oC.

Plots of θ against the logarithm of inhibitor concentration (log C_{inh}) for the three TU compounds at 30 ^oC are depicted in Fig. 3. The intercept of the obtained linear relationship is equal to $K_{ads,}$ which is related to the standard free energy of adsorption (ΔG^o_{ads}) by the following equation [20,23]:

$$K_{ads} = \frac{1}{55.5} exp \frac{-\Delta G^o_{ads}}{RT} \quad (6)$$

where 55.5 is the molar concentration of water in the solution (=1000/18 mol L^{-1}), R is the universal gas constant and T is the absolute temperature. It can be deduced from the positive slopes of the lines in Fig. 3 that there is a repulsion force in the compact adsorption layer since $a < 0$, i.e. has negative values computed as: -0.20, -0.23 and -0.38 for inhibitor TU-I, TU-II and TU-III on carbon steel. The corresponding K_{ads} values obtained from those linear plots are 8.85×10^5, 6.16×10^5 and 6.44×10^4 M^{-1}, respectively. As it is generally accepted, K_{ads} denotes the strength between the adsorbate and adsorbent, hence the above calculated values imply that TU-I and II are both more liable for adsorption on the metal surface than TU-III. In the meantime, the corresponding calculated ΔG^o_{ads} values are,

respectively as follows: - 44.61, -43.73 and -38.01 kJ mol^{-1} . These results indicate that the adsorption of the three tested inhibitors is a spontaneous process and that it is more feasible in the order: I > II > III in agreement with the trend of their inhibition or protection efficiency (cf. Table 1).

Generally, lower ΔG^{o}_{ads} values from -20 up to -40 kJ mol^{-1} are consistent with the electrostatic interaction between the charged molecules and the charged metal (physical adsorption). While ΔG^{o}_{ads} values more negative than -40 up to ~ -100 kJ mol^{-1} involve sharing or transfer of electrons from inhibitor molecules to the metal surface to form a coordinate type of bond (chemisorption) [35-37]. The values of ΔG^{o}_{ads} obtained were approximately equal to -42 ± 1 kJ mol^{-1}, indicating that the adsorption mechanism of the three tested thiouracil derivatives on carbon steel in 1.0 M H_2SO_4 solution involves both electrostatic adsorption and chemisorption [25]. The calculated thermodynamic parameters point toward both physisorption (major contributor) and chemisorption (minor contributor) of the inhibitors on the metal surface. The K_{ads} follow the same trend in the sense that large values of K_{ads} imply better and more efficient adsorption and hence better inhibition efficiency [24].

3.4. Effect of temperature

Corrosion reactions are usually regarded as Arrhenius processes, for which the rate (k) can be expressed by the relation [38]:

$$k = A\,exp(-\frac{E_a}{RT}) \tag{7}$$

where E_a is the activation energy of the corrosion process, R is the universal gas constant, T is the absolute temperature and A is the Arrhenius pre-exponential factor which depends on the metal type and electrolyte nature. Plots of log k vs $1/T$ for carbon steel in 1.0 M H_2SO_4 without and with the presence of 13 μM inhibitor (TU-I, TU-II or TU-III) are shown graphically in Fig. 4. The variation of log k vs $1/T$ is linear and the obtained E_a values from the slopes of those plots are summarized in Table 3. Compared with uninhibited solution, the increase of E_a in inhibited solution indicates that the energy barrier for the corrosion process increases and consequently its rate becomes sluggish. It is also indicated that the whole process is mainly controlled by the predominance of physical adsorption, without excluding also the week chemical bonding occurring between the inhibitor molecules and the carbon steel surface [25,39].

Table 3. Activation parameters of carbon steel dissolution in 1.0 M H_2SO_4 solution containing 1.3×10^{-5} M from each tested inhibitor.

Inhibitor	E_a (kJ mol^{-1})	ΔH^* (kJ mol^{-1})	$-\Delta S^*$ (J $mol^{-1}K^{-1}$)
Blank	48.6	45..9	119.7
TU-I	75.1	73.8	90.5

TU-II	72.7	70.3	82.6
TU-III	61.6	58.8	70.4

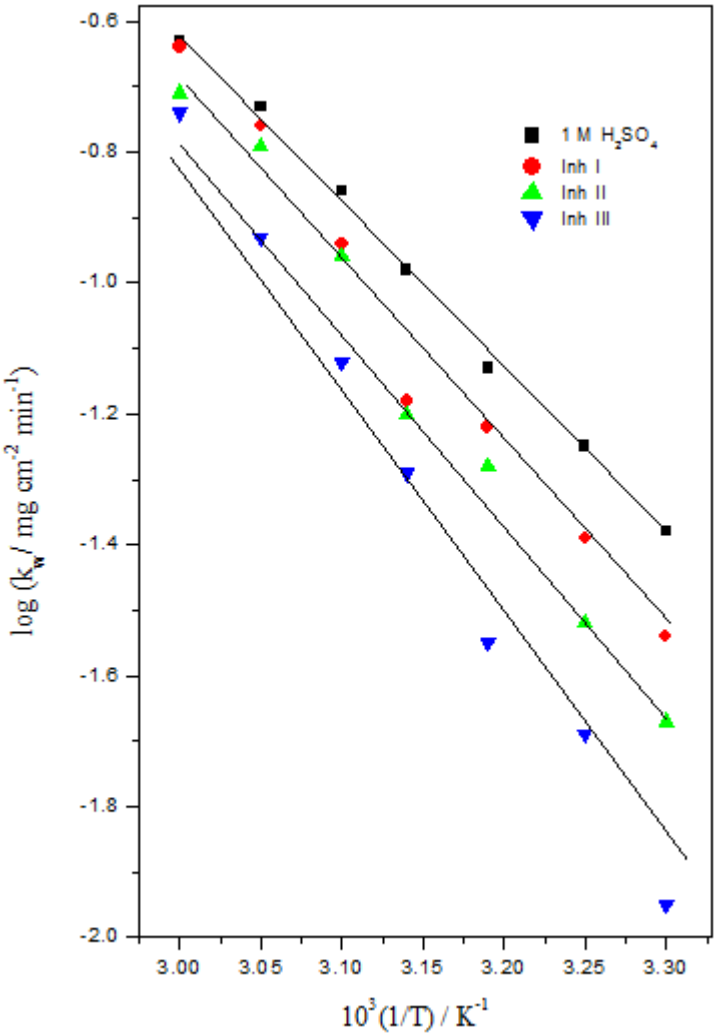

Figure 4. log k_w - (1/T) plots for carbon steel dissolution in 1.0 M H_2SO_4 alone or containing 13 μM from each of the three tested inhibitors.

Enthalpy and entropy of activation (ΔH^* and ΔS^*) can also be calculated based on the transition state theory using the following equation [40]:

$$k = \frac{RT}{Nh} exp(\frac{\Delta S^*}{R}) exp(\frac{-\Delta H^*}{RT}) \quad (8)$$

where *h* is Plank's constant, *N* is Avogadro's number. A plot of log *k*/*T* vs. 1/*T* gives also straight lines (not shown) for carbon steel dissolution in 1.0 M H_2SO_4 without and with 13μM of any inhibitor (TU-I, TU-II or TU-III). The slopes of those lines equal $\Delta H^*/2.303R$ and the intercepts equal {log (*RT/Nh*) + ($\Delta S^*/2.303R$)} from which the values of ΔH^* and ΔS^* were estimated and listed in Table 3. Inspection of these data reveal that the tested TU compounds act as inhibitors through increasing the activation energy of carbon steel dissolution by making a physical barrier to mass and charge transfer via their adsorption on the metallic substrate. Indeed, the positive enthalpy of activation (ΔH^*) reflects the endothermic nature for the formation step of the activated complex. On the other hand, the values of ΔS^* in the absence and presence of the tested compounds are large and negative, indicating that formation of the activated complex from reactants represents an association step rather than dissociation step. This means that a decreases in the system disorder takes place on going from reactants to activated molecules, which are in a state of higher order than the molecules at the initial state [20,41,42]. Generally, for the three tested inhibitors the order of the increase in E_a and ΔH^* and the decrease in ΔS^* remains the same as the order of their inhibition efficiency (TU-I > TU-II > TU-III).

3.5. Potentiodynamic polarization

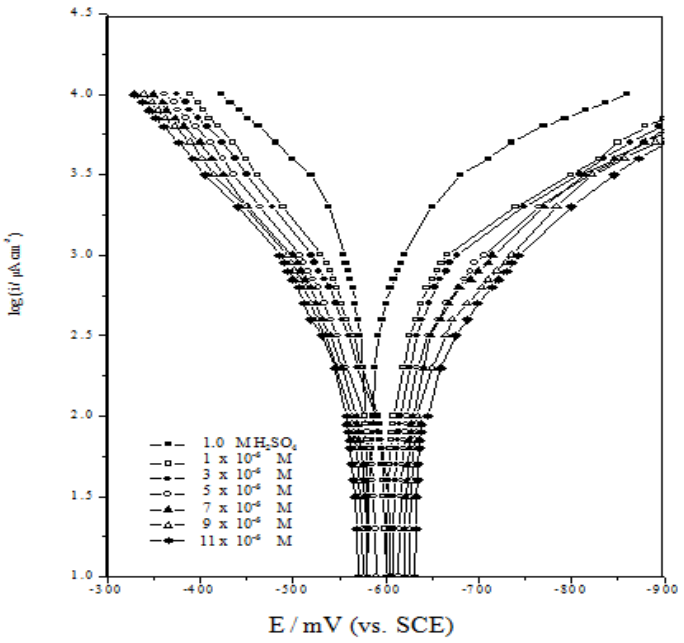

Figure 5. Potentiodynamic polarization curves for carbon steel in 1.0 M H_2SO_4 alone or containing different concentrations from TU-II inhibitor.

Tafel polarization curves (*E*-log*i*) for carbon steel were recorded in 1.0 M H_2SO_4 solutions containing various concentrations from inhibitors TU-I, TU-II and TU-III over the potential window of OCP ± 490 mV. Fig. 5 shows a typical example for TU-I, and similar behaviors are obtained for the other two (TU-II and TU-III). The important corrosion parameters and %*IE* calculated according to

Eq.(2) are given in Table 4. The results indicate that the cathodic and anodic curves obtained exhibit Tafel-type behavior.

Table 4. Potentiodynamic polarization and LPR parameters for corrosion of carbon steel in 1.0 M H_2SO_4 solution containing different concentrations from each tested inhibitor at 30 ^oC.

Inhibitor	[inhibitor] $\times 10^6$ (M)	$-E_{corr}$ (mV)	i_{corr} (mA cm^{-2})	$-\beta_c$ (mV dec^{-1})	β_a (mV dec^{-1})	R_p (ohm cm^2)	$\%IE_i$
Blank	0	530	11.0	240	200	4.0	-
TU-I	1	530	6.6	220	180	6.8	40
	3	525	6.0	240	180	7.5	45
	5	518	5.4	240	175	8.8	51
	7	517	4.3	210	175	11.5	61
	9	512	3.8	240	175	12.2	65
	11	512	2.7	240	175	17.8	75
	13	510	2.0	210	170	28	82
TU-II	1	530	7.7	243	210	6.0	30
	3	530	7.4	240	180	7.0	33
	5	530	6.3	230	175	8.2	43
	7	535	5.4	210	175	10.5	51
	9	520	4.1	200	180	11.2	63
	11	530	3.3	210	175	14.0	70
	13	525	2.9	220	180	15.3	74
TU-III	1	535	8.8	220	200	5.5	20
	3	530	8.3	240	190	6.8	25
	5	520	7.8	240	185	8.0	29
	7	518	6.6	210	185	9.8	40
	9	525	6.0	240	175	10.1	45
	11	515	4.9	240	185	12.0	55
	13	525	4.4	210	180	13.2	60

Additionally, the form of these curves is very similar either in the cathodic or in the anodic side, indicating that the mechanisms for both carbon steel dissolution and hydrogen reduction apparently remain unaltered in the presence of these additives. Therefore, addition of thiouracil compounds decreases the cathodic and anodic current densities and leading to parallel displacement of the cathodic and anodic curves to more negative and positive values, respectively. This means that the presence of thiouracil molecules in acid solution inhibits both the hydrogen evolution and the metal

dissolution processes with an overall shift of E_{corr} towards more negative values relative to the blank. The results also show that the slopes of the anodic and the cathodic Tafel lines (β_a and β_c) were slightly changed on increasing the concentration of the investigated compounds. This indicates that there is no change in the mechanism of inhibition in presence and absence of inhibitors. The fact that the values of β_c are slightly higher than β_a suggests a cathodic action of the inhibitor. This means that thiouracil derivatives are mixed type inhibitors, but the cathode is more preferentially polarized than the anode. The higher values of Tafel slope can be attributed to surface kinetic process rather than a diffusion-controlled process [23]. The almost constant value of ~ -240 mV dec^{-1} for the cathodic slope indicates that hydrogen evolution reaction is an activation controlled process [43], and that addition of thiouracil derivatives does not modify its mechanism. This result suggests that the inhibition mode of thiouracil derivatives used is by simple blockage of the surface via adsorption.

3.6. Linear polarization resistance (LPR)

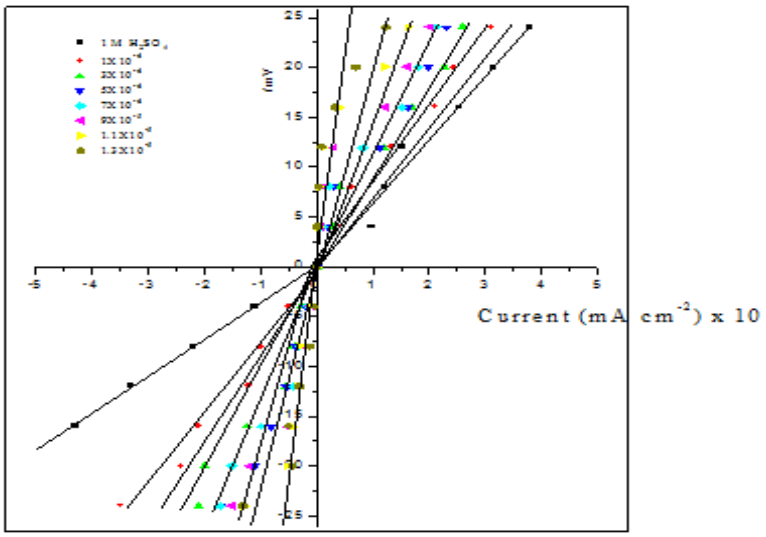

Figure 6. Linear polarization curves of carbon steel in 1.0 M H_2SO_4 alone or containing different concentrations from TU-II inhibitor at 30 ºC.

LPR values were obtained from *E-i* curves measured under low field of polarization in the domain of $\eta = \pm 25$ mV only. Fig. 6 is a typical experimental results obtained for carbon steel in 1.0 M H_2SO_4 solution alone or containing different concentrations from TU-I, and similar behaviors are obtained for the other two tested compounds. The slopes of those plots (LPR or R_p values) for the three tested thiouracils were estimated and listed also in Table 4. Generally, the values of R_p, and consequently the %*IE* increase with increase in concentrations of the added thiouracil derivative, indicating that these compounds act as efficient protection agents for carbon steel in sulfuric acid medium. For example, R_p value increases from 3.8 Ω cm^2 in the inhibitor free solution to 48 Ω cm^2 in the presence of 13 µM from TU-I. In the meantime at any given inhibitor addition, the trend in the R_p increase is in conformity with the above order, i.e. TU-I > TU-II > TU-III.

3.7. Electrochemical impedance spectroscopy

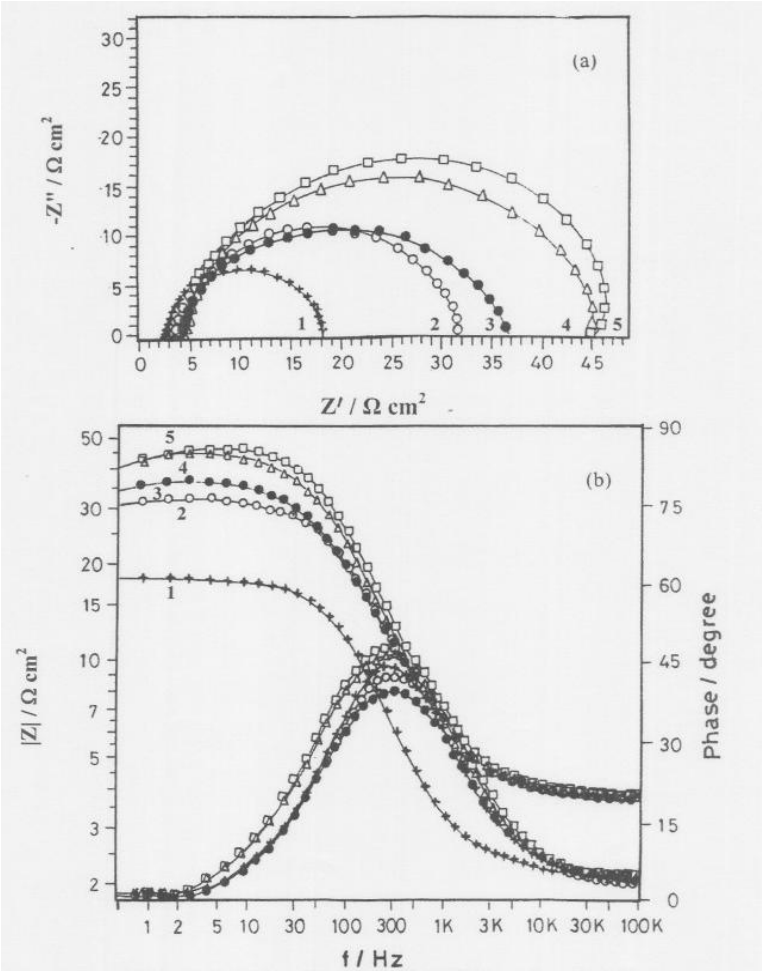

Figure 7. Impedance diagrams of carbon steel in 1.0 M H_2SO_4 alone or containing different concentrations from TU-III inhibitor at 30 ºC: (1) blank, (2) 1.0×10^{-6} M, (3) 5.0×10^{-6} M, (4) 9.0×10^{-6} M, (5) 1.3×10^{-5} M (a) Nyquist plots; and (b) Bode plots.

EIS is a powerful tool to evaluate the protective properties of organic additives on metal surface [44]. The impedance diagrams on Nyquist and Bode formats for carbon steel in 1.0 M H_2SO_4 solution alone or containing different concentrations from TU-I, TU-II and TU-III were traced over the frequency range 0.5 Hz-100 kHz at OCP. Fig. 7 illustrates a typical example for the results of TU-III compound at 30 ^{o}C, and similar curves were obtained for the other two. It is obvious that each spectrum of the Nyquist phase plots characterizes by a single full semicircle. The fact that impedance diagrams have an approximately single semicircular appearance indicates that the corrosion of carbon steel is controlled by a charge transfer process. Small distortion was observed in some diagrams, which has been attributed to frequency dispersion due to heterogeneity or roughness of the metal surface [45]. The equivalent circuit that describes the present metal/electrolyte corroding system is the simple Randles model shown in Fig. 8, where R_s, R_{ct} and C_{dl} refer to solution resistance, charge transfer resistance and the double layer capacitance of the interface, respectively. EIS parameters and %*IE* were calculated and listed in Table 5. On the Bode plots the absolute impedance ($|Z|$) at the high

frequency limits corresponds to R_s (Ω), while at the lower frequency limits corresponds to (R_{ct} + R_s). Therefore, the low frequency contribution shows the kinetic response of the charge transfer reaction [46]. Both of the diameter of the capacitive loop on the Nyquist plot and the absolute impedance (|Z|) at low frequency on the Bode plot increase with the rise in inhibitor concentration, which confirm a significant increase in the protection efficiency.

Table 5. Electrochemical corrosion parameters derived from EIS data for carbon steel after 30 min immersion in 1.0 M H_2SO_4 solution alone or containing different concentrations from each inhibitor at 30 ^oC.

Inhibitor	[inhibitor] $\times 10^6$ (M)	R_{ct} (ohm cm^2)	C_{dl} (μF cm^{-2})	%IE_R
Blank	0	18	86	-
TU-I	1	30	76	40
	5	40	60	55
	9	54	50	66
	13	68	42	73
TU-II	1	22.7	70	36
	5	26.5	57	50
	9	50.0	48	60
	13	60.5	40	65
TU-III	1	19.2	45	28
	5	20.3	40	40
	9	22.3	28	50
	13	45.6	40	60

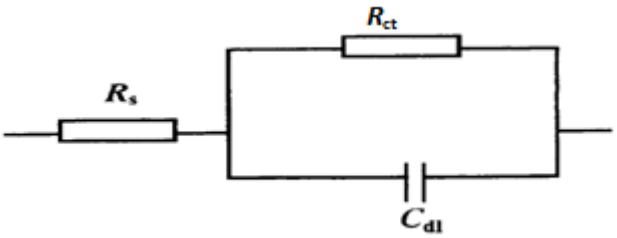

Figure 8. Electrical equivalent circuit of the corroding system.

Inspection of the EIS data presented in Table 5 reveals that R_{ct} increases and C_{dl} decreases with increasing inhibitor concentration. The increase in R_{ct} values, and consequently the inhibition efficiency refers to more impediment of the active area at the metal surface. This may be due to the gradual replacement of water molecules by the adsorbed inhibitor molecules to form an adherent film

on the metal surface as a result of increasing inhibitor concentration. On the other hand, the decrease in C_{dl} values can be described according to the Helmholtz model in which the double layer capacitance is inversely proportional to the surface charges [47,48]: $C_{dl} = \varepsilon_o\varepsilon/d$, where d is the film thickness, ε_o is the permittivity of air and ε is the local dielectric constant. It follows that the decrease in C_{dl} values indicates a decrease in the local dielectric constant or an increase in the thickness of the electrical double layer. Hence, the addition of TU molecules may adsorb at the electrode surface by replacing the water molecules. At the same inhibitor concentration, the values of R_{ct} comply with the order of TU-I > TU-II > TU-III, leading to the same trend for the inhibition efficiency. These results again confirm that the three tested TU compounds exhibit good inhibitive performance for carbon steel in sulfuric acid solution, and that 6-methyl-2-thiouracil is more efficient to protect the carbon steel corrosion than the other two derivatives. It is worth noting that the impedance data are in good agreement with the inhibition behavior of the inhibitors obtained from other techniques.

3.8. Quantum chemical calculations

Quantum chemical studies have been usually implemented to correlate the corrosion protection efficiency of organic inhibitors with their calculated molecular orbital energy levels [20,49,50]. Therefore, some parameters such as the energies of molecular orbital, E_{HOMO} (energy of the highest occupied molecular orbital), E_{LUMO} (energy of the lowest unoccupied molecular orbital), the energy gap ($\Delta E = E_{HOMO} - E_{LUMO}$), and the dipole moment (μ) were calculated based on *Ab initio* MO calculations method [51]. E_{HOMO} is often associated with the electron donating ability of the molecule, i.e. its ionization potential (IP). High values of E_{HOMO} indicate a tendency of the molecule to donate electrons to appropriate acceptor molecules with low energy and empty molecular d orbital of a metl. It is known that the electronic configuration of Fe atom is: [Ar] $4s^2 3d^6$, and 3d orbital is not fully filled with electrons. The unfilled 3d orbital could bind with the HOMO of the inhibitors [52,53], whereas the filled 4s orbital could donate the electron to LUMO of the inhibitors, since E_{LUMO} indicates the ability of the molecule to accept electrons, i.e. its electron affinity (*EA*) [54,55].

The inhibition efficiency (%*IE*) increases with decreasing E_{HOMO}, i.e. with decreasing the ionization potential ($IP = - E_{HOMO}$), and with increases E_{LUMO} or the electron affinity (*EA*) of the compound ($EA = - E_{LUMO}$) [56]. Another point regarding MO energy level is the energy gap (ΔE) between HOMO and LUMO for TU derivatives, which can be used as a characteristic important stability index for metallic complexes [49]. So that, a large ΔE value implies high stability for the molecule in chemical reactions [57]. Therefore, as MO gap energy increases the efficiency of a compound to inhibit the corrosion process increases, which reflects the experimental findings (cf. Table 6). Additionally, for the dipole moment (μ) displayed in the last column of Table 6, higher value of μ will favor the enhancement of corrosion inhibition as documented by Zhang et al. [58]. It follows that more CH_3-TU molecules adsorb on the surface, leading to higher protection performance for carbon steel corrosion in sulfuric acid.

3.9. Corrosion inhibition mechanism

From the previous results of various experimental techniques used, it was concluded that the tested thiouracil derivatives (CH_3-TU, TU and ph-TU) inhibit the corrosion of carbon steel in 1.0 M H_2SO_4 by adsorption at the metal/solution interface. The essential effect of these compounds as corrosion inhibitors is due to the presence of free electron pairs in the sulfur and the nitrogen atoms, π-electrons on the aromatic and thiouracil rings, molecular size and the formation of metallic complexes. The unshared and π-electrons interact with d-orbital of steel to provide a protective film. The inhibitive properties of such compounds depend on the electron densities around the chemisorption centre, in the sense that higher electron density at the centre means more effective inhibitor. The following explanations are postulated for the order of the investigated compounds which was found experimentally to be as follows: CH_3-TU > TU > ph-TU**.**

Table 6. Some quantum chemical parameters for the studied three compounds.

Inhibitor	$-E_{HOMO}$ (eV)	E_{LUMO} (eV)	$-\Delta E$ (eV)	μ
TU-I	8.925	2.524	11.449	6.09
TU-II	9.034	2.397	11.431	5.39
TU-III	9.062	1.434	10.496	2.03

Thiouracil interferes in the dissolution reaction via adsorption at the metal surface in two different ways. First, the inhibitor competes with $(SO_4)^{2-}$ ions for sites at the water covered anodic surface. In doing so, the protonated inhibitor loses its associated proton(s) before entering the double layer and chemisorbs by donating electrons to the metal. In the second way the protonated inhibitor adsorbs electrostatically onto the anion covered surface, through its cationic form. The thiouracil compounds exhibits corrosion inhibition efficiency as they are adsorbed through three active centers: the sulfur, oxygen and nitrogen atoms as shown in Fig. 9. The extent of adsorption, and thereby inhibition, was found to differ depending upon whether the substituent group was electron-releasing or electron-withdrawing. For instance, the presence of an electron releasing group is assumed to provide increased inhibitor efficiencies because it increases the electronic density on the active atoms in the compound. The effect is more pronounced if an aromatic moiety is present [59,60]. Among the present investigated compounds, TU-I derivative is found to give the best inhibition efficiency. This highest performance is likely attributed to the presence of methyl group (-CH_3) in its molecular formula, which is highly electron releasing group leading to greater increase in the electron density on its molecular active centers. Additionally, the π-electron interaction between the aromatic nucleus and the positively-charged metal surface play also an important role. This offers greater surface coverage, and consequently higher inhibition efficiency.

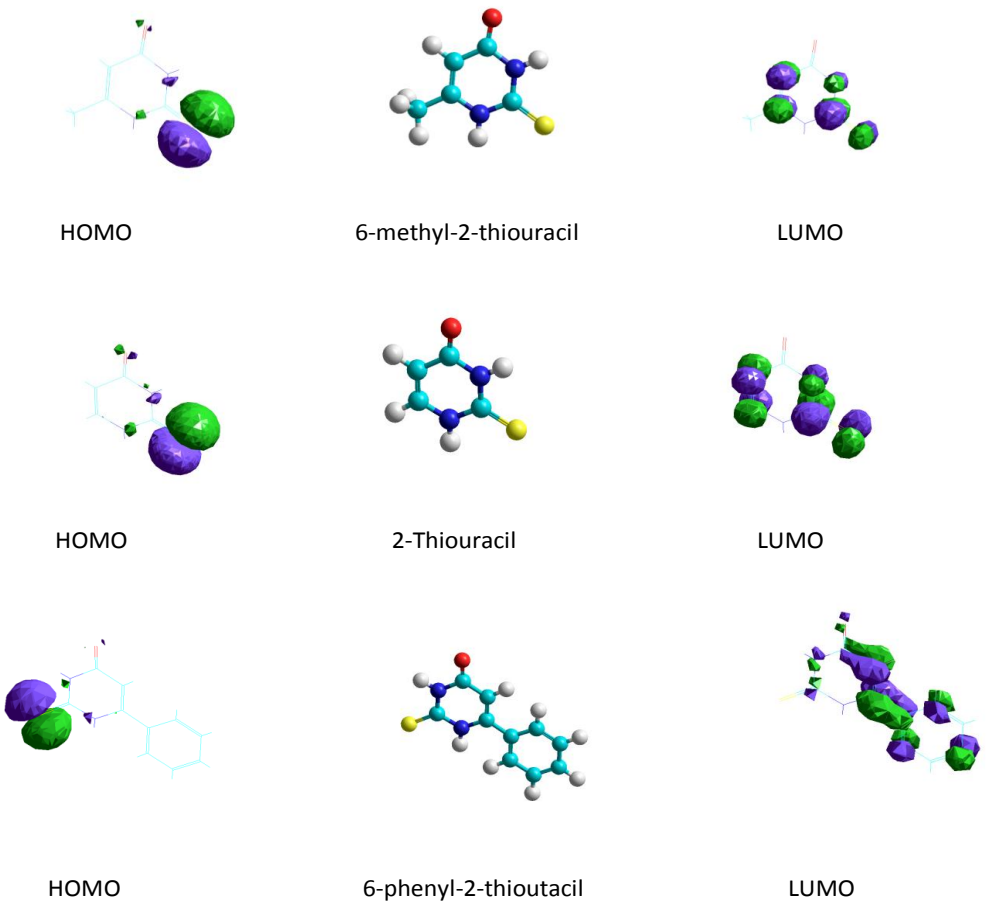

Figure 9. The optimized molecular structures and the molecular orbital (HOMO and LUMO) of the three studied inhibitors.

4. CONCLUSIONS

(1) The investigated thiouracil derivatives exhibit good inhibitive performance for carbon steel in 1.0 M H_2SO_4 by adsorption onto the metal surface.

(2) The %*IE* increases with either increase in inhibitor concentration or decrease in temperature. At all concentrations, %*IE* followed the order: CH_3-TU > TU > ph-TU**.** The compounds are of mixed type inhibitors, but the cathode is more polarized than the anode, i.e. they suppress both of anodic carbon steel dissolution and cathodic hydrogen gas evolution reactions.

(3) Adsorption of the three tested compounds obeys Temkin isotherm. The mechanism of the adsorption process is through physisorption (major contributor) and chemisorption (minor contributor) onto the metal surface. The negative high value of ΔG°_{ads} obtained from this study indicates that these compounds are spontaneously strongly adsorbed on carbon steel surface.

(4) A synergistic effect on *%IE* was observed by combination of each inhibitor with KI , KBr or KCl. At the same inhibitor concentration, the synergism is higher for KI and lower for KCl.

(5) The % *IE* obtained from weight loss, potentiodynamic and linear polarization curves, electrochemical impedance spectroscopy measurements, and quantum chemical calculations are all in good agreement.

ACKNOWLEDGEMENT
The authors gratefully acknowledge Professor H. Moustafa, Chemistry Department, Faculty of Science, Cairo University for running the software of quantum energy calculations.

References

1. E.P. Degarmo, J.T. Black, R.A. Kohser, Materials and Processes in Manufacturing (9th ed.), Wiley,USA, 2003.
2. H.H. Uhlig, R.W. Revie, Corrosion and Corrosion Control, Wiley, NewYork, 1985.
3. A.M. Alsabagh, M.A. Migahed, S.A. Hayam, *Corros. Sci.*, 48 (2006) 813 - 828.
4. V.S. Sastri, Corrosion Inhibitors - Principles and Applications, Wiley, Chichester, England, 1998.
5. G. Trabanelli, *Corrosion*, 47 (1991) 410 - 419.
6. M. El Achouri, M.R. Infante, F. Izquierdo, S. Kertit, H.M. Gouttoya, B. Nciri *Corros. Sci.*, 43 (2001) 19 - 35.
7. Z. Aitchikh, D. Chebabe, A. Dermai, N. Hajjaji, A. Srhiri, M.F. Montemor, M.G.S. Ferreira, A.C. Bastos, *Corros. Sci*., 47 (2005) 447 - 459.
8. J.M. Bastidas, J.L. Polo, E. Cano, *J. Appl. Electrochem.*, 30 (2000) 1173 - 1177.
9. S. Muralidharan, K.L.N. Phani, S. Pitchumani, S. Ravichandran, S.V.K. Iyer, *J. Electrochem. Soc*., 142 (1995) 1478 - 1483.
10. Z. Zhang, S. Chen, Y. Li, L. Wang, *Corros. Sci*., 51 (2009) 291-300.
11. S.M.A. Hosseini, A. Azimi, *Corros. Sci.*, 51 (2009) 728 - 732.
12. M. Lebrini, C. Roos, H. Vezin, F. Robert, *Int. J. Electrochem. Sci*., 6 (2011) 3844 - 3857.
13. F. Bentiss, M. Lebrini, M. Traisnel, M. Lagrenee, *J. Appl. Electrochem*., 39 (2009) 1399-1407.
14. L. Tang, X. Li, L. Li, Q. Qu, G. Mu, G. Liu, *Mater. Chem. Phys.*, 94 **(**2005) 353 - 359.
15. F. Bentiss, M. Traisnel, M. Lagrenee, *Corros. Sci*., 42 (2000) 127 - 146.
16. F. Bentiss, M. Lebrini, H. Vezin, F. Chai, M. Traisnel, M. Lagrenee, *Corros. Sci*., 51 (2009) 2165 - 2173.
17. N.E. Hamner, in: C.C. Nathan (Ed.), Corrosion Inhibitors, NACE Houston, Texas, USA, 1973, p. 1.
18. M. Ajmal, M.A.W. Khan, S. Ahmad, M.A. Quraishi, Heterocyclics as Corrosion Inhibitors for Acid Media in: A. Raman, P. Labine (Eds.), Reviews on Corrosion Inhibitor Science and Technology, vol. 2, NACE International, Houston, TX, 1996, Iv-1 to Iv-21.
19. W. Machu, 3rd European Symposium, Corrosion Inhibitors, University of Ferrara Italy, Ferrara, Italy, 1971, p. 107.
20. F. El-Taib Heakal, A. Fekry, *J. Electrochem. Soc*., 155 (2008) C534 - C542.
21. H. Zarrok, A. Zarrouk, B. Hammouti, R. Salghi, F. Bentiss, *Corros. Sci*., 64 (2012) 243-252.
22. A.A. Farag, M.A. Hegazy, *Corros. Sci.*, 74 (2013) 168 - 177.
23. A.S. Fouda, F. El-Taib Heakal, M.S. Radwan, *J. Appl. Electrochem*., 39 (2009) 391- 402.
24. A. Khamis, M.M. Saleh, M.I. Awad, *Corros. Sci*., 66 (2013) 343-349.
25. X. Li, S. Deng, H. Fu, X. Xie, *Corros. Sci.*, 78 (2014) 29-42.
26. K. Aramaki, N. Hackerman, *J. Electrochem. Soc*., 116 (1969) 568-574.

27. L. Larabi, Y. Harek, M. Traisnel, A. Mansri, *J. Appl. Electrochem.*, 34 (2004), 833 - 839.
28. S.A. Uneron, O. Ogbobe, I.O. Igwe, E.E. Ebenso, *Corros. Sci*., 50 (2009) 1998-2006.
29. K. Aramaki, M. Hagiwara, H. Nishihara, *Corros. Sci.*, 27 (1987) 487-497.
30. K. Aramaki, *Corros. Sci.*, 44 (2002) 871-886.
31. F. Bentiss, M. Bouanis, B. Mernar, M. Traisnel, M. Lagrenee, *J. Appl. Electrochem*.,32 (2002) 671-678.
32. R.M. Tennet (Ed.), Science Data Book, Oliver and Boyd, Edinburgh,1978, vol. 56.
33. G.N. Mu, X.M. Li, G.H. Liu, *Corros. Sci.*, 47 (2005) 1932-19-52.
34. M.G. Hosseini, H. Khalilpur, S. Ershad, *J. Appl. Electrochem*., 40 (2010) 215-223.
35. E. Bensajjay, S. Alehyen, M. El Achouri, S. Kertit, *Anti-Corros. Meth. Mater*., 50 (2003) 402-409.
36. S.Z. Duan, Y.L. Tao, Interface Chem. Higher Education Press, Beijing, 1990, 124.
37. B.B. Damaskin, O.A. Petrij, V.V. Batrakov, Adsorption of organic compounds on electrodes, Plenum Press, New York, 1971.
38. J.M. Deus, B. Díaz, L. Freire, X.R. Nóvoa, *Electrochim. Acta*, 131 (2014) 106-115.
39. B. Xu, W. Yang, Y. Liu, X. Yin, W. Gong, Y. Chen, *Corros. Sci.*, 78 (2014) 260-268.
40. F. El-Taib Heakal, A.S. Fouda, M.S. Radwan, *Int. J. Electrochem. Sci.*, 6 (2011) 3140- 3163.
41. S. Martinez, I. Stern, *Appl. Surf. Sci.*, 199 (2002) 83-89.
42. F. El-Taib Heakal, A.S. Fouda, M.S. Radwan, *Mater. Chem Phys*., 125 (2011) 26-36.
43. A. El-Ouafi B. Hammouti, H. Oudda. S. Kerit, R. Touzani, A. Ramdani, *Anti-Corros. Meth. Mater*., 49 (2002) 199-204.
44. F. El-Taib Heakal, S. Haruyama, *Corros. Sci*., 20 (1980) 887-898.
45. F. Mansfeld, M.W. Kendig, S. Tsai, *Corrosion*, 38 (1982) 570-580.
46. F. Mansfeld, *Eletrochim. Acta*, 35 (1990) 1533-1544.
47. E. McCafferty, N. Hackerman, *J. Electrochem. Soc.*, 119 (1972) 146-154.
48. E. McCafferty, Introduction to corrosion science, Springer, New York, 2010.
49. A. Kosar, M.H. Moayed, A. Davoodi, R. Parvizi, M. Momeni, H. Eshghi, H. Moradi, *Corros. Sci.*, 78 (2014) 138-150.
50. G. Gece, S. Bilgic, *Corros. Sci*., 52 (2010) 3435-3443.
51. H. Moustafa, S. El-Taher, M.F. Shibl, R. Hilal, *Int. J. Quant. Chem*., 87 (2002) 378-388.
52. P. Zhao, Y. Li, Q. Liang, *Appl. Surf. Sci*., 252 (2005) 1596-1607.
53. B.M. Mistry, S.K. Sahoo, S. Jauhari, *J. Electroanal. Chem*., 704 (2013) 118-129.
54. H.F. Finley, N. Hackerman, *J. Electrochem. Soc.*, 107 (1960) 259-263.
55. H. Ju, Z. Kai, Y. Li, *Corros. Sci.*, 50 (2008) 865-871.
56. V.S. Sastri, J.R. Perunareddi, *Corrosion*, 53 (1997) 671-678.
57. G. Gece, *Corros. Sci*., 50 (2008) 2981-2992.
58. J. Zhang, J. Liu, W. Yu, Y. Yan, L. You, L. Liu, *Corros. Sci*., 52 (2010) 2059-2065.
59. Y. Xiao-Ci, Z. Hong, L. Ming-Dao, R. Hong-Xuan, Y. Lu-An, *Corros. Sci*., 42 (2000) 645-653.
60. K.F. Khaled, N. Hackerman, *Electrochim. Acta*, 48 (2003) 2715-2723.